

A Single-species Atomic Co-magnetometer Based on ^{87}Rb atoms

Zhiguo Wang^{1,2*}, Xiang Peng^{3*}, Rui Zhang⁴, Hong Guo^{3†}, Hui Luo^{1,2†}, Jiajia Li¹, Zhiqiang Xiong¹, Shanshan Wang¹

1 College of Advanced Interdisciplinary Studies, National University of Defense Technology, Changsha, 410073, P R China

2 Interdisciplinary Center of Quantum Information, National University of Defense Technology, Changsha 410073, P R China

3 State Key Laboratory of Advanced Optical Communication Systems and Networks, School of Electronics Engineering and Computer Science, and Center for Quantum Information Technology, Peking University, Beijing 100871, P R China

4 College of Liberal Arts and Sciences, National University of Defense Technology, Changsha, 410073, P R China

Abstract: The co-magnetometer has been one of the most sensitive device to test new physics related to spin-dependent interactions. But the co-magnetometers based on overlapping ensembles of different spin species usually suffer from systematic errors resulting from magnetic field gradients. Here we propose a co-magnetometer based on the Zeeman transitions of the two hyperfine levels in the ground state ^{87}Rb atoms. It shows nearly negligible sensitivity to the variations of laser power and frequency, magnetic field, and magnetic gradients. In the preliminary experiment, it holds the potential to reach 10^{-17} eV level for measuring the hypothetical spin-dependent gravitational energy of the proton. Moreover, its performance can be further improved through optimization of the ^{87}Rb cell and experiment setup.

PACS: 07.55.Ge, 32.60.+I, 32.10.Fn

I Introduction

The spin-precession frequency of atoms has been one of the most sensitive means for testing fundamental physical effects, including EDM [1-5], CPT- and Lorentz-violation [6-8], and exotic spin-dependent interactions [9-11]. A recent systematic review on the test of these new physical effects can be found in [12]. The magnetic field variation is a severe factor that limits the accuracy in devices based on spin-precession, since spins have very strong interactions with magnetic field. In order to solve this problem, various co-magnetometers are proposed, which use spins overlapping in the same space to common-mode suppress the magnetic field variation [2-11]. There are still, however, several systematic errors reducing the magnetic field variation suppression capability in the co-magnetometers [13, 14]. Nearly all the co-magnetometers work on gas or liquid atoms, which move randomly in the vessel. Because of the slow and different diffusion rates of different spin species, there exists some spatial separation between the ensemble-averaged position of different spin

species [13]. As a result, the magnetic field cannot be common-mode suppressed effectively in the presence of magnetic field gradient. Moreover, the co-magnetometers based on gas spin usually utilize spin-exchange optical pumping technique to polarize the spins, which could cause some problems, such as frequency shift of Zeeman transitions. For example, in co-magnetometers based on alkali metal and dual noble gas spins (Rb- $^{129}\text{Xe}/^{131}\text{Xe}$, Rb- $^{129}\text{Xe}/^3\text{He}$, etc.), polarized alkali metal atoms exert different effective magnetic fields on the noble gas spins, leading to systematic errors [9]. Several methods are proposed to overcome this kind of problem. Dividing the pumping and probing into two separate phases and measuring the spin-precession of ^3He and ^{129}Xe in the dark could reduce the influence of polarized Rb atoms to a great extent [15]. Operating the $^{129}\text{Xe}/^{131}\text{Xe}$ spins with synchronous pumping could also reduce the frequency shift effect caused by the polarized Rb atoms [16]. But the above two methods work at the cost of complex manipulation of the spins. In a co-magnetometer based on $^{85}\text{Rb}/^{87}\text{Rb}$ contained in an evacuated coated cell, the influence of magnetic field gradient can be greatly suppressed due to fast diffusion rate of gas atoms [17-19]. But the magnetic-field-gradient shift cannot be eliminated ideally since the shift is proportional to gyromagnetic ratio squared while the gyromagnetic ratios of ^{85}Rb and ^{87}Rb are different [20, 21]. Besides, the pumping light leads to systematic error due to effects such as scattering and light shift. Therefore, careful calibration for effects caused by pumping light and probe light is needed [17-19]. In order to eliminate the systematic errors caused by magnetic field gradient, a co-magnetometer with identical molecules is proposed [14], which shows great performance to magnetic field variation and magnetic field gradient suppression. But the polarization and detection of the nuclear spin in molecules make the system very complex.

In this paper, we propose a new co-magnetometer based on the hyperfine levels of ^{87}Rb in an evacuated, paraffin-coated cell. It is operated with only a linearly polarized laser beam perpendicular to a bias magnetic field. Thanks to the nearly identical gyromagnetic ratio of the two hyperfine levels and identical diffusion coefficient, the co-magnetometer shows extremely small dependence on the magnetic field gradient.

In addition, it has negligible light shift on Zeeman transition frequency, since the tensor light shift due to linearly polarized light does not cause central frequency shift on Zeeman transitions. Even though there is a little residual circularly polarized component in the probe light which will cause vector light shift, its influence is very small because the propagating direction is perpendicular to the bias magnetic field. In our experiment, we obtain excellent magnetic field variation suppression and extremely small magnetic field gradient effect. In the preliminary experiment, the potential accuracy of the spin-gravity interaction test is comparable to the most sensitive co-magnetometer in the present.

II Experiments and Results

The configuration of the co-magnetometer is shown in Fig. 1. In this experiment, we use a single-beam double-resonance-alignment-magnetometer configuration [22, 23]. The key component is a glass cell with 20 mm in diameter and paraffin coating in the internal surface, which was made by Peking University. Beneficial to the paraffin coating, the linewidth of Rb Zeeman spectrum can be as narrow as about 2 Hz. A static bias magnetic field B_0 along z axis and an orthogonal driving magnetic field B_x oscillating at f are applied. A 25 μ W linear polarized laser beam, nearly resonant with the ^{87}Rb D_2 $F = 1 \rightarrow F'$ transition, is used to polarize the ^{87}Rb atoms and to probe the evolution of the atomic polarization. The magnetic resonance process can be understood in three steps, i.e. preparation, evolution and probing. At first, the laser beam creates second order polarizations (alignments) in both the $F=1$ and $F=2$ hyperfine levels of the ground state of the ^{87}Rb atom. Because the Larmor frequency of B_0 is much larger than relaxation rate of the atomic polarization, only the alignment components along B_0 remain, while other alignment components relax to zero quickly. And then, under the combined actions of the bias field B_0 , driving field B_x , and relaxation processes, the alignment precesses around B_0 at driving frequency f . When f equals to Larmor frequency of either one of the hyperfine levels, the alignment of corresponding hyperfine level comes to magnetic resonance. At last, the precessing alignments of both hyperfine levels modulate the polarization of the laser beam, which is detected by the polarimeter composed of a HWP, a PBS and a

balanced detector. All the experiments were done in the ambient temperature.

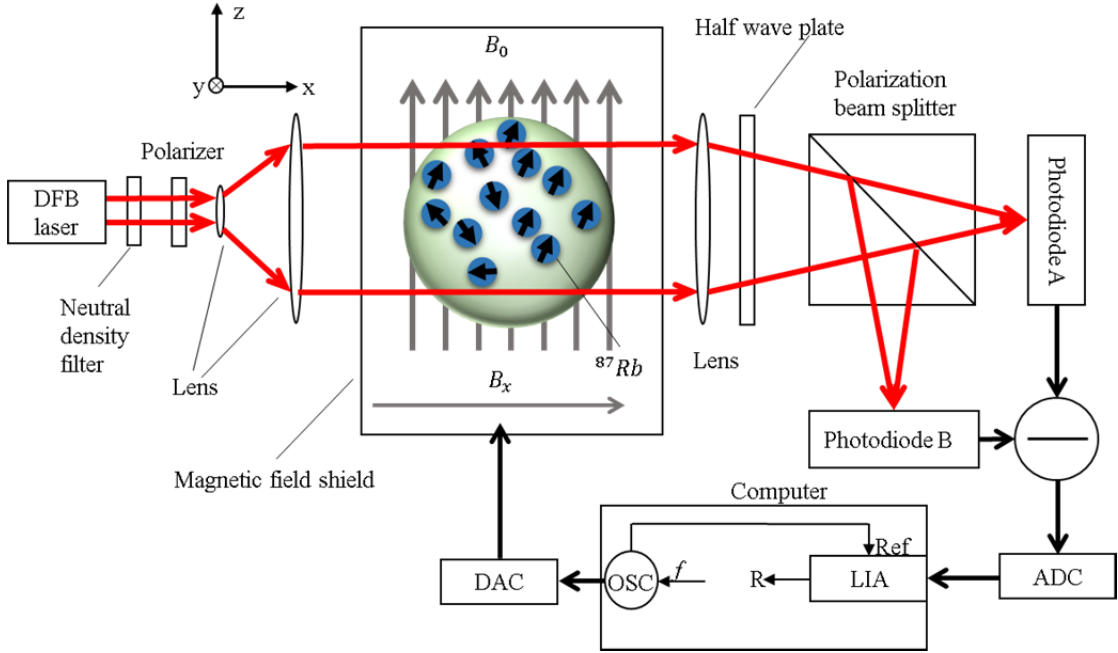
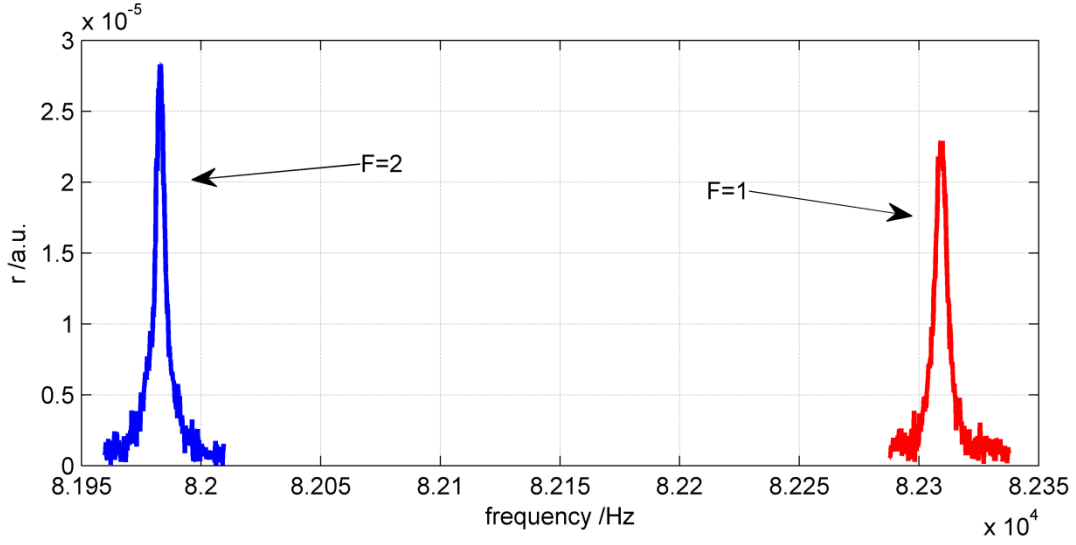


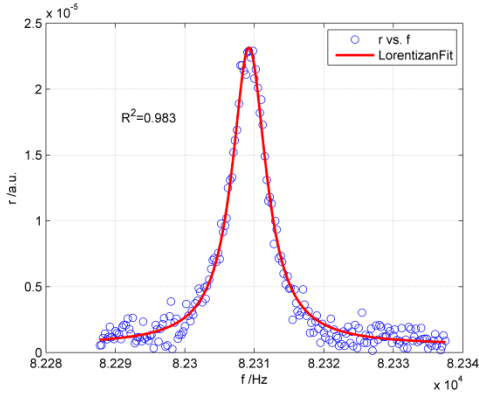
Fig. 1 (color online). Experimental setup. A spherical glass cell filled with an excess of ^{87}Rb is placed in the magnetic field shield. A set of solenoids are used to produce the bias magnetic field in z direction and the driving magnetic field in x direction. The probe light from a DFB laser with 780 nm propagates through a linear polarizer and a collimator made with two lenses. The probe laser propagates through the cell and then is focused with a lens. A half wave plate (HWP), a polarization beam splitter (PBS) and a balanced detector made up of two photodiodes are used to detect the paramagnetic Faraday rotation signal. The difference of the two photodiodes' signal is digitalized through an analog-to-digital converter (ADC). The output of an oscillator (OSC) is sent to a digital-to-analog converter (DAC) and then drives the x coil to produce oscillating magnetic field B_x . We obtain the Zeeman spectrum of the Rb atoms through scanning the frequency of B_x and recording the R channel of a lock-in amplifier (LIA) made with LabviewTM program. The amplitude of the driving field is about 0.1 nT and the frequency is changed linearly in the scan process.

The Zeeman spectrum at $B_0 \approx 11.79 \mu\text{T}$ is shown in Fig. 2(a). The frequency difference for the Zeeman transitions at two hyperfine levels in ground state is 326.4Hz, since the gyromagnetic ratios are different for the two hyperfine levels. The frequency ratio of them is $\gamma_2/\gamma_1 = 0.996033924$ in theory [24], where γ_2 and γ_1 are the gyromagnetic ratio for $F=2$ and $F=1$ respectively and the Larmor precession directions of these two hyperfine levels are opposite. The resonant frequency for each hyperfine level is obtained through fitting the resonance curve with a Lorentzian profile, as shown in Fig. 2(b) and 2(c). Since the Zeeman transition frequencies of the

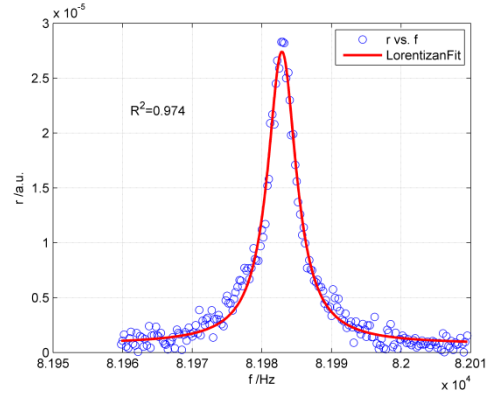
two hyperfine levels are both proportional to magnetic field, they can be used as a co-magnetometer.



(a)



(b)



(c)

Fig. 2 (color online). Zeeman spectroscopy of ^{87}Rb atoms at $11.79\mu\text{T}$ (a) and their fitting curves with Lorentzian profile for $F=2$ (b) and $F=1$ (c). The gyromagnetic ratio of the $F=1$ hyperfine level in ground state is $\gamma_1 = 7023.69 \text{ Hz}/\mu\text{T}$ and that of $F=2$ is $\gamma_2 = 6995.83 \text{ Hz}/\mu\text{T}$. As a result, they can be distinguished clearly. The Zeeman spectroscopy is a bit asymmetry because the scanning is a transient process.

We change the laser power through a neutral density filter and change the laser frequency through tuning the electric current flowing in the DFB laser diode, so that the influence of these laser parameters are obtained. The transverse relaxation time of the Rb spins is about 60 ms according to the resonance curve in Fig. 1 and it takes about 1 s to scan through the resonance peak, so the spins are not in equilibrium. As a result, the scanning curve is not an ideal Lorentzian profile. Taking this error into

account, we used a group of 4 phases to get a value, as shown in Fig. 3. The normalized frequency ratio (NFR), that is, $\nu_2/\nu_1 - 0.996033924$, as a function of laser frequency and power, is shown in Fig. 4. It should be noted that the Zeeman spectroscopy of the two hyperfine levels does not always appear. The NFR is on the order of 10^{-7} in the range of -4GHz to 3 GHz. The dispersion of NFR at $450\mu\text{W}$ is a bit larger than that at $200\mu\text{W}$. This may be due to the residual light shift. But as a whole, the NFR show a low sensitivity to variation of laser frequency and power.

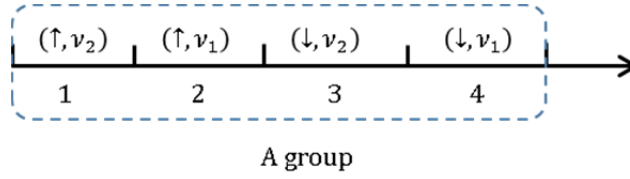


Fig. 3. The arrow direction denotes the scan direction, \uparrow for low frequency to high frequency, and \downarrow for high frequency to low frequency. The average frequency of phase 1 and 3 gives ν_2 and that of phase 2 and 4 gives ν_1 . Each phase takes 15 seconds.

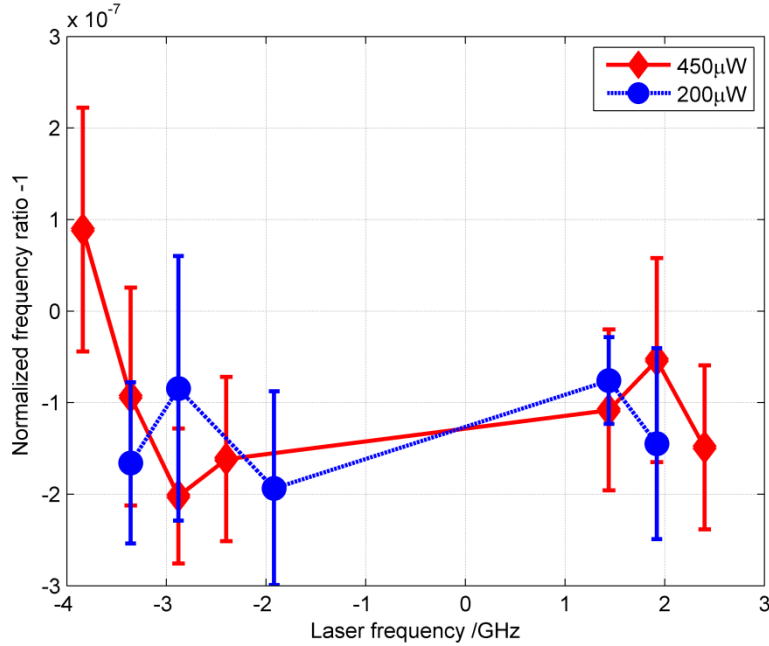


Fig. 4 (color online). NFR as a function of laser frequency and power. The laser frequency is shifted relative to the transition from $F=1$ branch of the ^{87}Rb D_2 line. The laser frequency is tuned from -4 GHz to 3 GHz with a step frequency of 0.48 GHz. At some frequencies, only one Zeeman peak appeared so the frequency ratio cannot be obtained. We did the experiment at two different laser power, which is

measured at the entrance hole of the magnetic field shield.

In order to check the ability of the co-magnetometer to suppress magnetic field variation, we measured NFR at different B_0 , as shown in Fig. 5. We did not find any trend of NFR on magnetic field, except fluctuations on the order of 10^{-7} due to measurement error. The factors such as nonlinear Zeeman Effect and asymmetry of the resonance curve could contribute to measurement errors at present. Nonlinear Zeeman Effect will results in deformation of the resonance curve. The errors above could be reduced through revising fitting profile and optimizing the parameter of the experiment system.

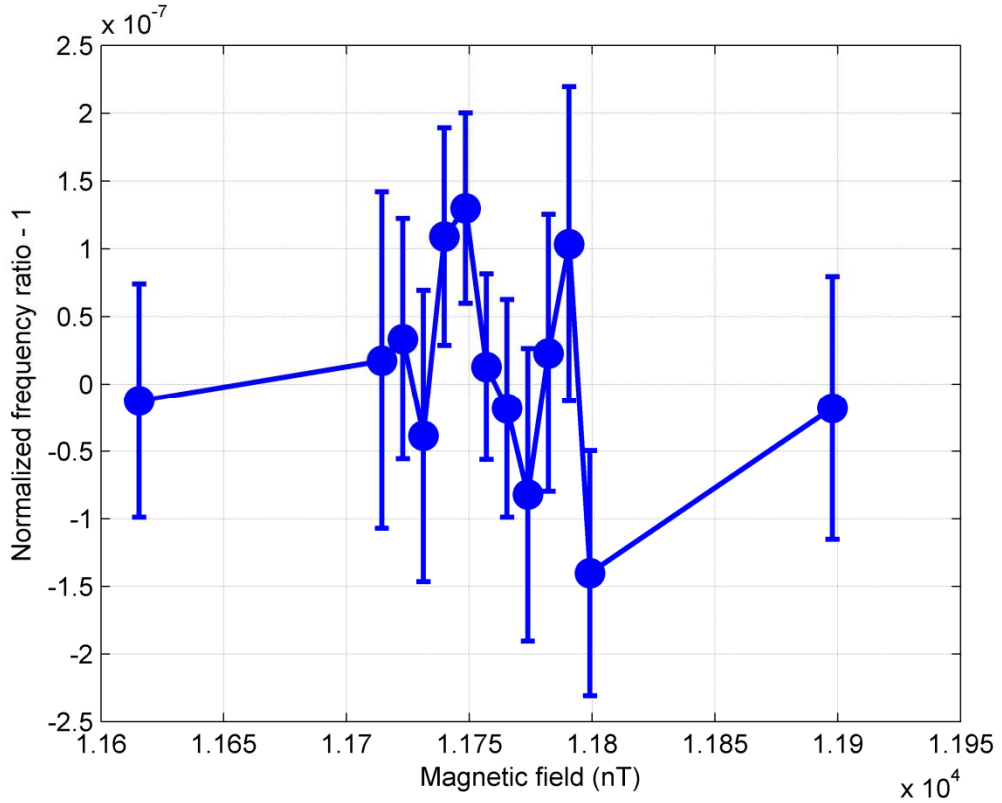


Fig. 5 (color online). NFR as a function of laser frequency and power. At first, we obtained the middle 11 points, which do not show trend of NFR on magnetic field. Therefore, we measured the NFR with a bit larger magnetic field variation, that is, the 2 points at the sides, which do not show trend of NFR on magnetic field, too.

Magnetic field gradient can lead to systematic errors in the co-magnetometers, especially for that using dual-species spins. For our co-magnetometer using only ^{87}Rb atoms, the magnetic-gradient effect resulting from the different-diffusion-rate is

nearly eliminated and the gyromagnetic ratio of the two hyperfine levels is almost identical. Therefore, we expect it is immune to magnetic field gradient. The NFR as a function of magnetic field gradient $\partial B_z / \partial z$ is shown in Fig. 6. It shows no apparent trend on magnetic field gradient, except fluctuations on the order of 10^{-7} .

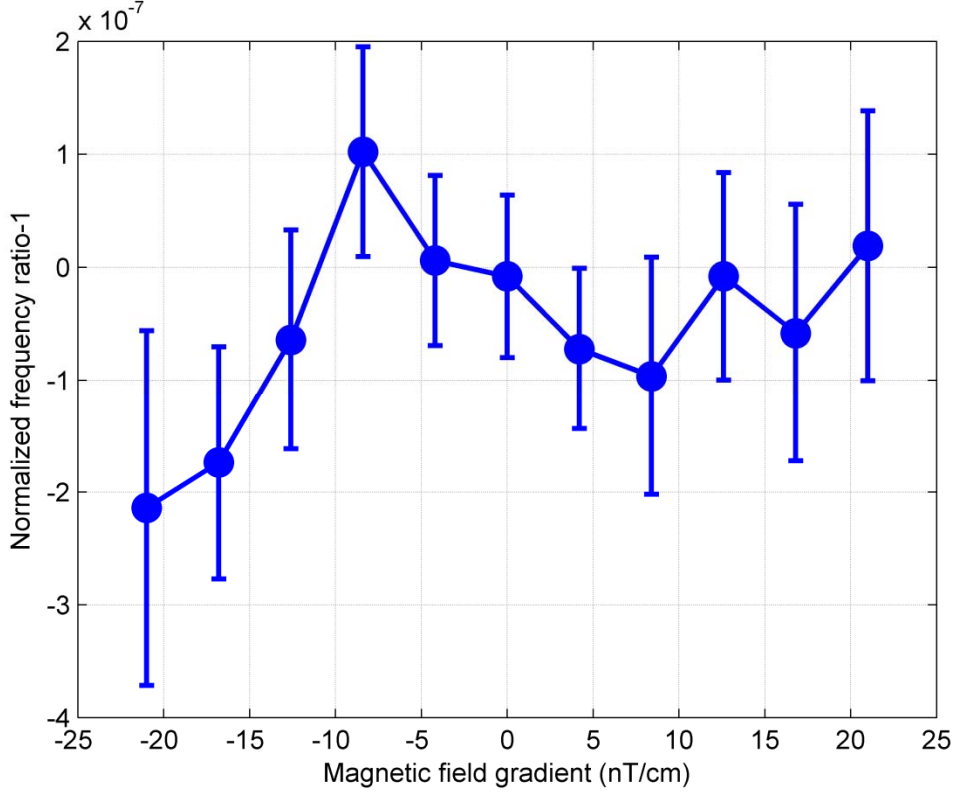


Fig. 6 (color online). Normalized frequency ratio as a function of magnetic field gradient $\partial B_z / \partial z$.

Because of the simplicity in structure and small systematic errors, our co-magnetometer is an ideal device for the test of fundamental physics, such as spin-gravity coupling. In [25], the gyrogravitational ratios of ^{87}Rb are given in the following equations,

$$\chi_{F=2} = 0.25\chi_e + 0.25\chi_p, \quad (2)$$

$$\chi_{F=1} = -0.25\chi_e + 0.42\chi_p. \quad (3)$$

where χ_e and χ_p are the gyrogravitational ratios of electrons and protons in ^{87}Rb atoms.

The spin-precession frequencies of the two hyperfine levels, are given by,

$$\nu_1(\pm) = \gamma_1 B_z \mp \chi_{F=1} \frac{g \cos \phi}{\hbar}, \quad (4)$$

$$v_2(\pm) = \gamma_2 B_z \pm \chi_{F=2} \frac{g \cos \phi}{\hbar} . \quad (5)$$

where “ \pm ” in $v_1(\pm)$ and $v_2(\pm)$ denotes reversing the magnetic field direction, g is the acceleration due to gravity, and ϕ is the angle between the bias magnetic field B_z and Earth’s gravitational field. The opposite signs of $\chi_{F=1}$ and $\chi_{F=2}$ terms in the right hand sides of (4) and (5) derive from the opposite Larmor-precession directions of the $F=1$ and $F=2$ hyperfine levels. We construct the ratio,

$$R_+ = \frac{v_2(+)}{v_1(+)} = \frac{\gamma_2 B_z + \chi_{F=2} \frac{g \cos \phi}{\hbar}}{\gamma_1 B_z - \chi_{F=1} \frac{g \cos \phi}{\hbar}} , \quad (6)$$

$$R_- = \frac{v_2(-)}{v_1(-)} = \frac{\gamma_2 B_z - \chi_{F=2} \frac{g \cos \phi}{\hbar}}{\gamma_1 B_z + \chi_{F=1} \frac{g \cos \phi}{\hbar}} . \quad (7)$$

The difference of the ratio through reversing the magnetic field B_z is,

$$\Delta R = R_+ - R_- \approx \frac{1.34 \chi_p g \cos \phi}{\gamma_1 B_z \hbar} . \quad (8)$$

Since in our experiment setup, the B_z is orthogonal to gravity, giving $\cos \phi = 0$, we cannot conduct the spin-gravity coupling test at present. However, we could estimate the potential sensitivity. We use 8 phases to obtain one set of data so as to reduce the transient effect in the scanning process, as shown in Fig. 7. In the experiment, we got 2882 groups. The measured ΔR sequences are shown in Fig. 8(a). We made a test of normality for ΔR , as shown in Fig. 8(b) and an Allan variance analysis for ΔR , as shown in Fig. 8(c). According to the data, we could obtain $\Delta R = 1(3) \times 10^{-8}$, corresponding to spin-dependent gravitational energy of the proton at a level of $3(10) \times 10^{-18}$ eV.

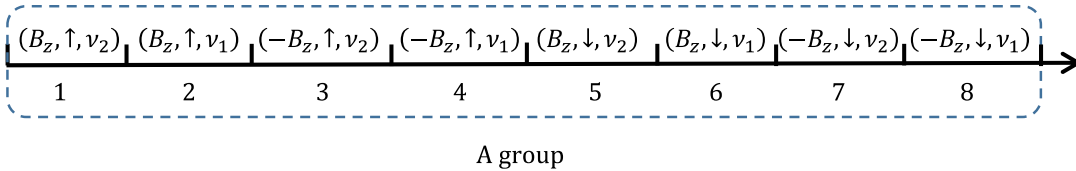


Fig. 7 The arrow direction denotes the scan direction, \uparrow for low frequency to high frequency, and \downarrow for high frequency to low frequency. The average frequency of phase 1 and 5 gives $v_2(+)$ and that of phase 2 and 6 gives $v_1(+)$ and it is the same rule for reverse B_z . Each phase takes 15 seconds. The magnetic field has a setup time of about 3s after reversing the direction.

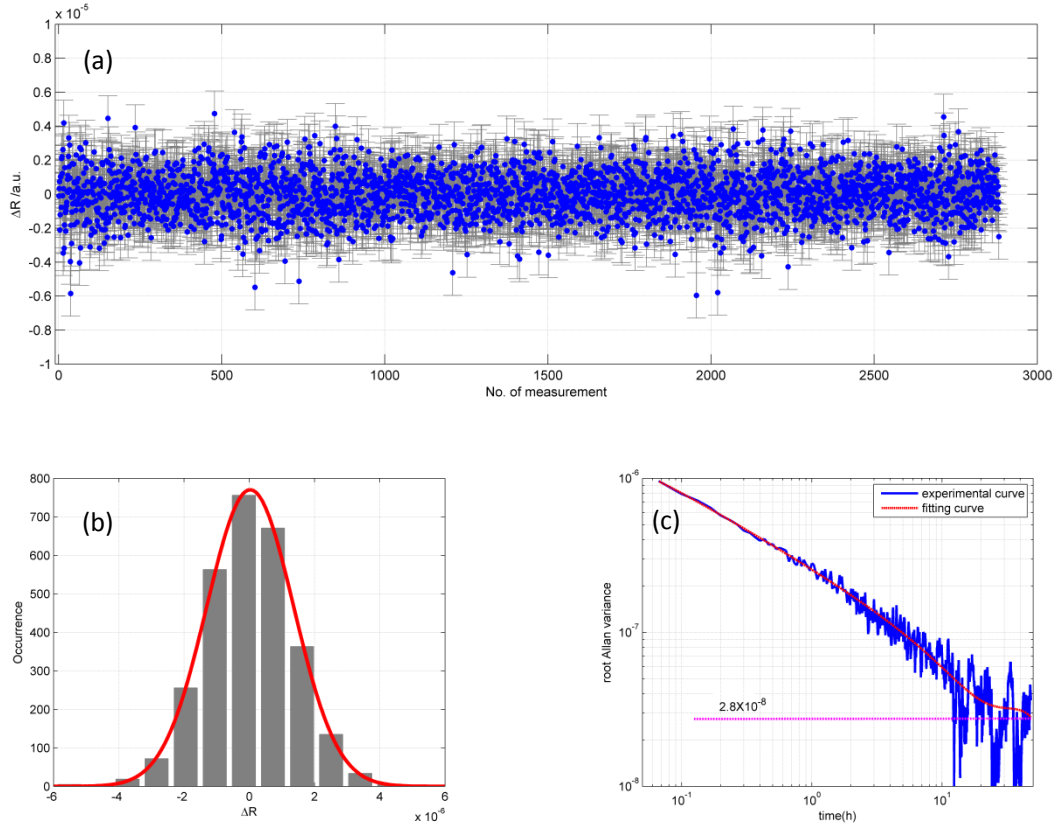


Fig. 8 (color online). Sensitivity estimates for a spin-gravity coupling measurement. (a) The calculated ΔR based on the measured R_{\pm} ; (b) Histograms of the measured ΔR with a Gaussian fitting which shows the measured ΔR sequence obeys a Gaussian distribution; (c) Allan variance analysis for measured ΔR sequence which shows the stability of ΔR reaches a floor of about 2.8×10^{-8} .

III Discussion

The ^{87}Rb co-magnetometer has fewer sources of systematic errors essentially. Compared with co-magnetometers using dual-species, its sensitivity to magnetic field gradient is extremely small. Compared with the co-magnetometer using ^{85}Rb and ^{87}Rb , the magnetic gradient related frequency shift is further suppressed, and the light shift is also suppressed with the help of linearly polarized laser beam used in the experiment. Compared with nuclear-spin co-magnetometer based on a liquid of identical molecules, it does not need extra magnetometer to read out the spin-precession frequency. Moreover, it runs well in ambient temperature.

There are still some problems in the co-magnetometer that limit its performance currently. (a) In order to reduce residual polarization effect of probe light, we set the laser power to below 1mW. The signal-to-noise ratio (SNR) is only about 20 in the present experiment system, which is somewhat low compared with other

co-magnetometers. (b) We use the scanning method to find the resonance frequency, which takes 15s to scan through one resonance frequency. As a result, the magnetic field noise in B_z cannot be common-mode suppressed effectively. (c) The scan curve of the resonance line has deformation to some degree, which leads to error in determining the resonance frequency based on the fitting the scan curve to a Lorentzian profile.

In order to improve the performance of the co-magnetometer, the following methods could be useful. (a) The linewidth of Zeeman transition can be narrowed further. In [26], a Rb cell with relaxation time about 60 s is reported, which gives potential to narrow the linewidth to the order of 0.1Hz. This may reduce the frequency determination error by 1~2 orders. (b) If we operate the Rb spin as a closed-loop spin oscillator, the SNR and magnetic field noise rejection capability could be improved greatly. (c) The gyromagnetic ratios of ^{85}Rb for the two hyperfine levels are also different. If both ^{85}Rb and ^{87}Rb or even more kind of alkali atoms are used to form dual co-magnetometers in a cell, some advantage may be obtained. For example, one can realize co-magnetometers to search for spin-gravity couplings using various combinations of protons and electrons.

In order to realize reliable test of fundamental physics, we have some plans except the sensitivity improvement. Due to the simple configuration, the co-magnetometer can be made very compact. Therefore, it is possible to locate several co-magnetometers at different places and different directions with gravity to test the fundamental physics in a long time. And it is also possible to form a co-magnetometer array so as to suppress some common-mode errors.

The co-magnetometer also has some other potential applications. Due to its lack of pumping frequency shift, the co-magnetometer may be used as a magnetometer for magnetic field measurement with an absolute accuracy of the order of 10^{-7} . With the co-magnetometer, we could also measure the g-factor ratios for alkali atoms [27].

IV Conclusion

In conclusion, we realized a new kind of co-magnetometer based on the Zeeman transitions in ground state hyperfine levels of ^{87}Rb atoms. It has very simple structure,

but it demonstrated excellent ability to suppress the magnetic field variation and extremely small systematic error caused by magnetic field gradient. Preliminary experiments show that it is competitive to the most sensitive device in spin-gravity coupling measurement at present. Through further improvements on the system, such as narrowing the linewidth of Zeeman resonance spectrum, enhancing the SNR, and making the ^{87}Rb atoms to be continuous masers, the sensitivity could be improved greatly. After these improvements, a compact, high-precision system can be realized for long-term spin-dependent exotic interactions.

V Acknowledgement

This research was supported by the Natural Science Foundation of China (61671458, 61571018, 61571003, 91436210), Research Project of National University of Defense Technology (ZK18-02-04), and Natural Science Foundation of Hunan Province (2018JJ3608).

*These authors contributed equally to this work.

†Corresponding author. Email: hongguo@pku.edu.cn (H.G.); luohui.luo@163.com (H.L.)

References

- [1] A. Yoshimi, K. Asahi, K. Sakai, M. Tsuda, K. Yogo, H. Ogawa, and M. Nagakura, "Nuclear spin maser with an artificial feedback mechanism," *Phys. Lett. A* **304**, 13 (2002).
- [2] T. E. Chupp, R. J. Hoare, R. L. Walsworth, and B. Wu, "Spin-exchange-pumped ^3He and ^{129}Xe Zeeman masers," *Phys. Rev. Lett.* **72**, 2363 (1994).
- [3] M. A. Rosenberry and T. E. Chupp, "Atomic electric dipole moment measurement using spin exchange pumped masers of ^{129}Xe and ^3He ," *Phys. Rev. Lett.* **86**, 357 (2001).
- [4] C. Abel et al., "Search for axionlike dark matter through nuclear spin precession in electric and magnetic fields," *Phys. Rev. X* **7**, 041034 (2017).
- [5] T. Sato, Y. Ichikawa, S. Kojima, C. Funayama, S. Tanaka, T. Inoue, A. Uchiyama, A. Gladkov, A. Takamine, Y. Sakamoto, Y. Ohtomo, C. Hirao, M. Chikamori, E. Hikota, T. Suzuki, M. Tsuchiya, T. Furukawa, A. Yoshimi, C.P. Bidinosti, T. Ino, H.

Ueno, Y. Matsuo, T. Fukuyama, N. Yoshinaga, Y. Sakemi, and K. Asahi, “Development of co-located ^{129}Xe and ^{131}Xe nuclear spin masers with external feedback scheme,” *Phys. Lett. A*, **382**, 588 (2018).

[6] F. Allmendinger, W. Heil, S. Karpuk, W. Kilian, A. Scharth, U. Schmidt, A. Schnabel, Yu. Sobolev and K. Tullney, “New limit on Lorentz-invariance- and CPT-violating neutron spin interactions using a free-spin-precession ^3He - ^{129}Xe comagnetometer,” *Phys. Rev. Lett.* **112**, 110801 (2014).

[7] V. A. Kostelecký and C. D. Lane, “Constraints on Lorentz violation from clock-comparison experiments,” *Phys. Rev. D* **60**, 116010 (1999).

[8] J. M. Brown, S. J. Smullin, T.W. Kornack, and M. V. Romalis, “New limit on Lorentz- and CPT-Violating neutron spin interactions,” *Phys. Rev. Lett.* **105**, 151604 (2010).

[9] M. Bulatowicz, R. Griffith, M. Larsen, J. Mirijanian, C. B. Fu, E. Smith, W. M. Snow, H. Yan and T. G. Walker, “Laboratory search for a long-range T-Odd, P-Odd interaction from axionlike particles using dual-species nuclear magnetic resonance with polarized ^{129}Xe and ^{131}Xe gas,” *Phys. Rev. Lett.* **111**, 102001 (2013).

[10] G. Vasilakis, J. M. Brown, T. W. Kornack and M. V. Romalis, " Limits on new long range nuclear spin-dependent forces set with a K-He-3 comagnetometer," *Phys. Rev. Lett.* **103**, 261801 (2009).

[11] K. Tullney, F. Allmendinger, M. Burghoff, W. Heil, S. Karpuk, W. Kilian, S. Knappe-Grüneberg, W. Müller, U. Schmidt, A. Schnabel, F. Seifert, Yu. Sobolev, and L. Trahms, “Constraints on Spin-Dependent Short-Range Interaction between Nucleons,” *Phys. Rev. Lett.* **111**, 100801 (2013).

[12] M. S. Safronova, D. Budker, D. DeMille, D. F. Jackson Kimball, A. Derevianko, and C. W. Clark, “Search for new physics with atoms and molecules,” *Rev. Mod. Phys.* **90**, 025008 (2018).

[13] D. Sheng, A. Kabcenell and M. V. Romalis, “New classes of systematic effects in gas spin comagnetometers,” *Phys. Rev. Lett.* **113**, 163002 (2014).

[14] T. Wu , J. W. Blanchard, D. F. J. Kimball, M. Jiang, and D. Budker, “Nuclear-spin comagnetometer based on a liquid of identical molecules,” *Phys. Rev. Lett.* **121**,

023202 (2018).

[15] M. E. Limes, D. Sheng, and M. V. Romalis, “ ^3He - ^{129}Xe Comagnetometry using ^{87}Rb Detection and Decoupling,” *Phys. Rev. Lett.* **120**, 033401 (2018).

[16] A. Korver, D. Thrasher, M. Bulatowicz, and T. G. Walker, “Synchronous spin-exchange optical pumping,” *Phys. Rev. Lett.* **115**, 253001 (2015).

[17] D. F. Jackson Kimball, I. Lacey, J. Valdez, J. Swiatlowski, C. Rios, R. Peregrina-Ramirez, C. Montcrieffe, J. Kremer, J. Dudley, and C. Sanchez, “A dual-isotope rubidium comagnetometer to search for anomalous long-range spin-mass (spin-gravity) couplings of the proton,” *Ann. Phys. (Berlin)* **525**, 514 (2013).

[18] D. F. J. Kimball, J. Dudley, Y. Li, D. Patel, and J. Valdez, “Constraints on long-range spin-gravity and monopole-dipole couplings of the proton,” *Phys. Rev. D*, **96**, 075004 (2017).

[19] J. Mora, A. Cobos, D. Fuentes, and D. F. J. Kimball, “Measurement of the ratio between g-factors of the ground states of ^{87}Rb and ^{85}Rb ,” arXiv 1809.04053v1 (2018).

[20] G. D. Cates, W. Happer and S. R. Schaefer, “Relaxation of spins due to field inhomogeneities in gaseous samples at low magnetic fields and low pressures,” *Phys. Rev. A*, **37** 2877 (1988).

[21] J. M. Pendlebury, J. M. Pendlebury, W. Heil, Yu. Sobolev, P. G. Harris, J. D. Richardson, R. J. Baskin, D. D. Doyle, P. Geltenbort, K. Green, M. G. D. van der Grinten, P. S. Iaydjiev, S. N. Ivanov, D. J. R. May, and K. F. Smith, “Geometric-phase-induced false electric dipole moment signals for particles in traps,” *Phys. Rev. A*, **70**, 032102 (2004).

[22] A. Weis, G. Bison and A. S. Pazgalev, “Theory of double resonance magnetometers based on atomic alignment,” *Phys. Rev. A*, **74** 033401 (2006).

[23] S. J. Ingleby, C. O’ Dwyer, P. F. Griffin, A. S. Arnold, and E. Riis, “Vector magnetometry exploiting phase-geometry effects in a double-resonance alignment magnetometer,” *Phys. Rev. Appl.* **10**, 034035 (2018).

[24] Daniel A. Steck, “Rubidium 87 D Line Data,” available online at <http://steck.us/alkalidata> (revision 2.1.5, 13 January 2015).

[25] D. F. Jackson Kimball, “Nuclear spin content and constraints on exotic

spin-dependent couplings,” *New J. Phys.* **17**, 073008 (2015).

[26] M. V. Balabas, T. Karaulanov, M. P. Ledbetter, and D. Budker, “Polarized alkali-metal vapor with minute-long transverse spin-relaxation time,” *Phys. Rev. Lett.* **105**, 070801 (2010).

[27] C. W. White, W. M. Hughes, G. S. Hayne, and H. G. Robinson, “Determination of g-factor ratios for free Rb^{85} and Rb^{87} atoms,” *Phys. Rev.* **174**, 23 (1968).